RSC Advances

ROYAL SOCIETY OF CHEMISTRY

www.rsc.org/advances

Quantum Mechanical Calculations of the Interactions Between Diazacrowns and the Sodium Cation: An insight into Na^+ Complexation in Diazacrown-Based Synthetic Ion Channels

A. A. Skelton[1]*, N. Agrawal[1] and J. R. Fried[2]

1. School of Health Sciences, Discipline of Pharmacy, University of KwaZulu-Natal, South Africa
2. Chemical Engineering, University of Louisville, Louisville, Kentucky, USA

Keywords: Quantum mechanical calculations, ion solvation, ion complexation

*corresponding author, skelton@ukzn.ac.za

Abstract

Quantum mechanical calculations were performed to study the conformational behavior and complexation between a sodium cation and a diazacrown (diaza-18-crown-6) using density functional theory (DFT), Møller-Plesset (MP2) and molecular mechanics methods. A goal of this work is to gain a fundamental understanding of the interplay between water molecules, the sodium cation and a diazacrown. Diazacrowns have a significant importance as the functional units of a synthetic sodium channel, called a hydraphile, which functions within a lipid bilayer.

This study follows on from our previous classical molecular dynamics study, which investigated the free energy of transport of Na^+ as it passes through a lipid bilayer. In the present study we focus on the complexation of Na^+, the conformation of the diazacrown and electronic structure that cannot be accessed by classical force fields. Furthermore, we benchmark the force field used in the previous study and make a modification of the dihedral parameters to improve its description. A whole range of configurations are scanned to gain an understanding of the energy landscape and find the minimum energies for configurations involving the diazacrown, diazacrown-Na^+, diazacrown-water and diazacrown-Na^+-water configurations.

Our results show that there is an attractive interaction between Na^+ and the oxygen and nitrogen atoms of the diazacrown for which the interaction between Na^+ and the oxygen atoms are the stronger of the two. Natural bond orbital (NBO) analysis shows charge-tranfer between the diazacrown and Na^+ resulting in a reduced positive charge for this cation. This charge transfer occurs directly and via a water-mediated mechanism and could be crucial to the action of the hydraphile sodium channel. Since, in our previous classical molecular dynamics work, it was shown that water molecules accompany Na^+ cations as they are transported through a lipid bilayer, while the cations are complexed to the diazacrown moiety of the hydraphile, we aim to better understand the structural, electronic structural and energetic implications of this complexation. Calculations of a water molecule interacting with the diazacrown show that the strongest interaction involves a bridging water molecule that forms hydrogen bonds with two diazacrown oxygen atoms or an oxygen and nitrogen atom on opposite sides of the diazacrown. These interactions may be important in the ordering of water to form a water channel that allows the Na^+ to pass through the lipid bilayer.

Introduction

A variety of synthetic ion channels, ranging from Calixarenes[1], peptidic macrocycles[2] and cyclodextrins[3] have been developed[4] with the aim to mimicking natural ion channels. Hydraphiles, a class of synthetic cation channels, have been found to possess antibacterial properties [5, 6] and attributed to them the ability to facilitate the transport of Na^+ across lipid membranes and, thereby, causing a disruption of bacterial cells[7-10]. A number of different hydraphiles[11] have been synthesized and the rate of Na^+ transport across a lipid bilayer has been found to be highly dependent on the combination of various functional groups that comprise the hydraphile[12-16]. Figure 1 shows a particular hydraphile that has been found to be one of the most effective sodium channels[17]. The lower panel of Figure 1 provides a representation of the current proposed model[18]. According to the current model, the hydraphile spans the lipid bilayer and Na^+ cations relay between diazacrowns with little movement of the diazacrowns themselves. This is based upon the observations that the rate of Na^+ transfer depends upon spacer length[19] and experimental evidence that hydraphile side arm groups, at the end of the hydraphile molecules, are located within the phospholipid head group region[20]. The diazacrowns must, therefore, complex Na^+ as an initial step for entry of Na^+ into the lipid bilayer. Furthermore, it has been suggested that the hydraphile acts as a channel by assisting with the reorganization of water, which in turn helps to solvate the Na^+ [21, 22]. This is based on the observation that the rate of Na^+ transfer is dependent of the size of the central diazacrowns of the hydraphile, which controls the number of configurations involving water molecules. Further insight into factors that can affect Na^+ transport can be provided through a combination of computational chemistry and molecular simulation techniques.

The first simulation study that investigated the hydraphile sodium channel was coarse grained simulation study concerning ion transport of the hydraphile within a lipid bilayer [23] has been reported. This study showed the entry of a coarse-grained Na^+-water cluster, represented by a single bead particle, was shuttled through the lipid bilayer via the diazacrowns of the hydraphile molecules. The coarse-grained study, however, did not provide the molecular and electronic detail that can elucidate how individual water molecules interact with the diazacrown and Na^+.

Recently, we published a study that investigated the full hydraphile within a lipid bilayer. In that study, the free energy of transport of the Na^+ through a DMPC lipid bilayer was studied. It was shown that there was a reduction of the free-energy of transport when the Na^+ was complexed with the diazacrown. The free energy with respect to the water coordination was calculated and it was shown that the free energy of water-desolvation of Na^+ was reduced by the presence of the hydraphile, in fact complexation by a terminal diazacrown. It was noticed that even when it was transported with the hydraphile, water molecules accompanied the Na^+. Figure 2 shows a snapshot from a molecular dynamics simulation of the Na^+ being pulled through a DMPC lipid bilayer whilst complexed with the terminal diazacrown of the hydraphile, two water molecules accompany the ion, one either side of the diazacrown molecule. We aim to gain an understanding of this effect on the level of detail that can be obtained by quantum mechanical calculations. The present study investigates the factors that control the complexation of the Na^+ within the diazacrown. One aspect is understanding the conformational preference of the diazacrown. If the lowest energy conformation of the diazacrown is quite different to that of the diazacrown when it is complexed to Na^+, the diazacrown will have to reorganize and this will cause an additional energy penalty to complexation. How will then water molecules interact with the diazacrown to help to reorganize the non-complexed diazacrown structure allowing it to be more susceptible to binding with Na^+?

Our choice to study this system with QM is for several reasons. First, we want to calculate with the most accurate energies and we benchmarked the DFT calculations with MP2/aug-cc-pvtz calculations. Since we are dissecting the thermodynamics of the diazacrown-complexation, it is most beneficial to use the most accurate calculations possible. This provides us with the most accurate geometries and interaction energies.

In this study, all quantum calculations will be compared with force field calculations. The force field in question is the force field used in our previous study. In that study, preliminary QM calculations were performed to compare the interaction energies between QM with the FF; however, these calculations did not deal with an adequately sampled conformational space, did not consider multiple configurations and did not consider the diazacrown-Na^+-water system. The geometric and electronic structural aspects such as intermolecular distances and NBO charges were also not analyzed in the previous study. The greater detail of the analysis in the present study will, therefore, highlight further whether the force field can adequately describe sodium complexation by the diazacrown within the lipid bilayer and bulk water.

To the best of our knowledge no QM studies of the complexation of Na^+ and diaza-18-crown-6 have been reported but many simulation studies have been made involving the complexation of crown ethers and their derivatives with ions. Many insights into the complexation and conformation of the crown ethers have been previously gained by quantum mechanical[24-38] and force field simulations[39-54]. These studies, due to the similarity of 18-crown-6 to the diaza-18-crown-6, provide us with a point of reference for comparison.

Specifically, in work by Al-Khahtani *et al*. [24], the binding energy of 18-crown-6 with Li^+, Na^+, K^+, Rb^+ and Cs^+ was calculated by HF, B3LYP, CAM-B3LYP, M06 and MP2 levels of theory. Behjatmanesh-Ardakani[25] used B3LYP to investigate aza-,diaza-, and triaza-12-crown-4 binding with Na+[25]. De *et al.*[28] simulated the complexation of many different crown ethers with Na^+ and Li^+ in the presence and absence of extra water molecule and Schurhammer *et al.*[33] studied different binding modes of water with 18-crown-6 using B3LYP [33].

In addition to studies of ions with crown molecules, many studies have used QM calculations to investigate the interaction between ions with water clusters[55-58]. It was shown that the structure of such clusters is a delicate competition between ion−water and water−water Interactions[59].

The hypothesis that water molecules interact with the hydraphile and assist in the action of the ion channel properties will be investigated[20-22, 60, 61]. Since it is unlikely that water molecules interact with the hydrocarbon part of the hydraphile, we should expect that the diazacrown is key in this respect and an understanding of how the water molecules form hydrogen bonds with the oxygen and nitrogen atoms of the diazacrown is a goal of this study.

One reason to use quantum mechanics to study this system is to monitor the electronic structure, particularly the charge transfer from the diazacrown to Na^+ since this could be a crucial effect in the hydraphile ion channel. Boda *et al*[26] showed by analysis of the HUMO-

LUMO gap, charge transfer of 12-crown-6 with Li^+. Varadwa et al[38] reported 18-azacrown-6 (all six oxygen atoms were substituted for nitrogen atoms) binding with late transition state metals and the observed, using NPA charges, the transfer of charge from the azacrown to the metal valence orbitals. Both studies showed that when more electron withdrawing substituents are use, the charge transfer increases.

One further objective is to investigate the importance of properly treating dispersion interactions to calculate interaction energies of highly interacting clusters. Calculations of interaction energies performed using DFT with the B3LYP functional[62], which is known for its poor treatment of dispersion interaction, will be reported. Results are compared with calculations using the ωB97XD functional[63], which provides superior treatment of dispersion interactions. MP2 calculations with a large basis set are used for further comparison.

Methodology/Quantum Mechanical Calculations

Density functional theory (DFT) calculations were performed on on diazacrown, diazarown-Na^+, diazarown-water and diazarown-water-Na^+ clusters using the 6-311+G(d,p) basis set with Gaussian 09[64]. DFT, using the density functional, B3LYP[62] and ωB97XD[63] was employed for geometry optimization. The ωB97XD functional was selected because of its superior ability to treat dispersion interactions[65].

Figure 4 illustrates the diazacrown used in the DFT calculations. In this study, nitrogen atoms in the diazacrown are terminated by a methyl group instead of a phenyl or hydrocarbon chain as in the case of the hydraphile.

One aspect of assessing the interaction between the diazacrown and Na^+ cation was to find the lowest energy configurations of the diazacrown and clusters of the diazacrown with a complexed Na^+. In addition, the minimum energy of the same complexed structure with the addition of water molecules was calculated to understand the effect of water molecules as they accompony the Na^+, as it is pulled through the lipid bilayer. Since the diazacrown is a large molecule and contains many degrees of freedom, the minimum cannot be necessarily obtained by simply performing a geometry optimization; doing so may result in the cluster being trapped within a local minimum. To counter this problem the distance between both nitrogen atoms and between two opposite oxygen atoms were constrained and systematically modified (scanned). Geometry optimizations were performed at each step completing a relaxed scan of the “opening” coordinates. The lowest energy configuration from both scans was re-optimized with no constraints.

Even though there are, obviously, other ways that the conformation of the diazacrown can be explored, we feel that adequate configuration space has been explored. We also performed scans of the various dihedrals within the diazacrown (results not shown), but since we obtained no extra configurations, we decided to omit those results for clarity.

Interaction energies between different diazacrown, water, and Na^+ interactions are reported. The interaction energies (E_{int}) were calculated in the following way:

$$E_{int}=E_{mol1\text{-}mol2}-E_{mol1}-E_{mol2}$$

where mol1 and mol2 are components of the complex. For example, in the water-Na^+ case, mol1 represents a water molecule and mol2 represents Na^+. Since the diazacrown alone and the diazacrown with two water molecules (no Na^+) need to minimized to calculate the interaction energy, these were also be scanned in the same way as the clusters involving Na^+.

Møller Plesset (MP2) calculations were also performed for the cluster. Geometry optimizations were performed using the 6-311G+(d,p) basis set and single point-energies were performed on the minimum energy structure using Dunning's augmented correlation consistent triple-zeta (aug-cc-PVTZ) basis set [66] to provide accurate energies. Frequency calculations were performed for the optimized geometries using DFT with the ωB97XD functional to calculate changes in enthaly (dH), free energy (dG) and entropy (dS). Changes in these values were given by taken by subtracting the components (mol1 and mol2) from the complex, as for the E_{int}, above.

The force field used in this study was the one used in our previous work[67] ;however, in that study, dihedral parameters were not included and in this case, when geometry-optimizations of the diazacrown were performed, there was a visible discrepancy between QM and force field geometries. For this reason the dihedral parameters were added. These dihedral parameters were taken from the MMFF force field [68] and validated by comparing the relative energies of different configurations of the diazacrown with different QM calculations. These parameters are shown in the Supplementary material (Table S1). Molecular mechanics calculations were performed using NAMD[69] to compare energies and force field-optimized geometries with QM calculations.

Results and Discussion

Conformational scans

As stated, scans of the N-N and O-O distances were performed for the diazacrown, diazarown-Na^+, diazarown-water and diazarown-water-Na^+ systems to investigate the effects of conformation and to find the lowest energy conformations.

The energy profiles of the scans are shown in Figure **3** and above the energy profiles is the diazacrown with the N-N and O-O distances indicated. Figure **3**a shows the scans with diazacrown only, Figure **3**b shows the diazacrown in the presence of the Na^+, Figure **3**c shows the diazacrown in the presence of two water molecules and Figure **3**d shows the diazacrown in presence of a Na^+ ion and two water molecules. The numbers on the graphs indicate different conformations that will be discussed. All the conformations that relate to the numbers are shown in the Supplementary material (Figures S1 to S5). Selected configurations that show unique conformations are shown in the manuscript, Figure **4**-Figure **8**.

Scans were also performed using the B3LYP functional and the lowest energy configurations were used in the B3LYP energy calculations. Scans were also made for the diazacrown in the presence of a single water molecule and the lowest energy was obtained from these scans.

Conformation of the diazacrown

The conformation of the diazacrown was investigated since this will influence its binding to Na^+. For example, if it is energetically favorable for the diazacrown to be in a closed position, it will have to rearrange to bind the Na^+ in a more open position.

Figure 4 shows the diazacrown in three different conformations. The numbers relate to numbers in the scan energy profiles in Figure 2a. Configuration 1 is the lowest energy configuration found by the scans using the ωb97xd functional. The arrows in the middle panel show the distances (N-N and O-O) that were scanned. The right panel shows the lowest energy configuration energy obtained from scans using the B3LYP functional. It was shown by Shurhammer at al [33] that there are three different forms of the 18-crown-6 crown ether; in that work, the C_i configuration is a more closed form and is similar to configuration 1 but with two of the nitrogen atoms in the diazacrown converted to oxygen atoms in the crown ether. The D_{3d} form is the open form and is similar to Configuration 7. There was a “mixed” form reported that was similar to the B3LYP optimized structure.

In Configuration 1, there are close contacts between hydrogen atoms and nitrogen atoms (at an average of 2.51 A) due to dispersion interactions. These interactions decrease the energy of this conformation. Configurations 3 to 5 in the Supplementary Information (Figure S1) show increasing levels of closing of the diazacrown and formation of intermolecular interactions and, therefore, lowering of the energy. The low energy configurations shown in Figure S2 (especially configuration 6), all have attractive hydrogen/oxygen intermolecular contacts and this also decreases the energy, relative to the more open structure.

Table 1 shows the relative energies of the three different structures, geometry optimized by

B3LYP, ωB97xd and MP2 using the 6-311G+(p,d) basis set. The MP2 energies were calculated using the aug-cc-pvtz basis set. For B3LYP, the mixed configuration is the lowest, closely followed by the closed, C_i configuration, followed by the open, D_{3d} configuration. For ωB97xd and MP2, however, the ordering is different, with the closed C_i (Configuration 1) being the lowest in energy, followed by the mixed (lowest B3LYP) with the open, D_{3d} (Configuration 7) structure being the highest in energy. The force field shows similar energies to the ωB97xd and MP2 energies validating our choice to improve the force field used in our previous work by adding extra dihedral parameters.

Interestingly the C_i configuration became more open when optimized by B3LYP and the hydrogen atom to nitrogen atom distance increased (3.16 Å), compared with ωB97xd (2.51 Å). The distance for MP2 is 2.54 Å, which is much more similar to the ωB97xd structure. Since, it is likely that the hydrogen atom to nitrogen atom interaction is due to dispersion interactions, this result shows how important dispersion interactions are; that is, the added dispersion terms in ωB97xd reproduce the MP2 result more closely (both in distance and the energetic ordering of the different configurations). The parentheses in Table 1 show the free energy values (the relative entropy, enthalpy and free energy values are shown in Table S2 in the Supplementary Materials). It can be noticed that the difference in free energy, between D_{3d} and C_i, is lower than the difference in energy. This is because there is less entropy (vibrational) in the Ci structure (lower by ~7 cal/mol/K) due to the hydrogen-nitrogen hydrogen bonds. This will reduce the favorability of this conformation.

Shurhammer *et al.* [33] showed that for the 18-crown-6, D_{3d} is less stable than C_i by 17 kcal/mol

(MP2/6-31G). We, however, found that for the diazacrown, (MP2/aug-cc-pvtz) the energy difference is only 7.35 kcal/mol. The difference in energy is due to the difference in basis set and because in the work of Shurhammer *et al* the crown ether was used instead of the diazacrown.

Conformation of Complexed diazacrown

Similar scans were performed for the diazacrown-Na^+ systems to investigate the effect of conformation on the binding. In the presence of Na^+, there is a barrier to changing the conformation away from the minimum. This is because the attraction of the nitrogen and oxygen atoms with Na^+ restricts large changes in N-N or O-O distances. There is a shoulder within the minimum energy for the N -N distance and this is responsible for the two different configurations (shown in Figure S3); however, these structures are qualitatively the same with only slightly different oxygen and nitrogen atom to Na^+ distances. The lowest energy configuration (configuration 2 in Figure **3**b) is shown in Figure **5**.

Conformation of diazacrown-water systems

The energy profiles in Figure 3c show the scans of the N-N and O-O distances when there are two water molecules but no Na^+ present. There are two low energy configurations, 1 and 4. Configurations 2 and 3 (Figure **6**b and S4) are similar to each other; these configurations have one water molecule that is bridging the diazacrown nitrogen atoms, hydrogen bonded with its hydrogen atoms (water N-N), and the other water molecule that is hydrogen bonded to the diazacrown oxygen with only one of its hydrogen atoms (water O). For configurations 1 (Figure **6**b) and 4 (Figure **6**c), however, both water molecules are bridging the diazacrown; for configuration 1, both water molecules are bridging a nitrogen and an oxygen atom (water N-O). For configuration 4 (Figure **6**c), one water molecule is bridging a nitrogen and an oxygen atom (water N-O) and the other water molecule is bridging two oxygen atoms (water O-O). Configurations 1 and 4 are the lowest energy configurations because all four water hydrogen atoms are hydrogen bonding with diazacrown nitrogen or oxygen atoms yet for configuration 3, only one water molecule has both of its hydrogen atoms hydrogen bonding, the other water molecule only hydrogen bonding with one of its hydrogen atoms. It can be noticed that the energy profiles of the diazacrown-water clusters are quite different to the diazacrown-only scans. Whereas in the diazacrown scans there is an energetic penalty for the diazacrown to be in a more open configuration, for the diazacrown-water scans the minima (Configurations 1-4) are at more open positions since open positions are necessary for water bridging to occur.

The diazacrown-water system with two water molecules was scanned to provide the lowest energy configuration to use in the interaction energy calculation of the diazacrown- water cluster. To provide a more lucid measure of the interaction energy between water and the diazacrown, however, relaxed scans of a diazacrown-water cluster, with only one water molecule, were performed.

Figure 7 shows two configurations that were obtained from the relaxed scans. Figure 7A shows the lowest energy configuration obtained from the scans using the ωb97xd functional; in this configuration the water is hydrogen-bonding with both diazacrown nitrogen atoms (N-N bridging). Figure 7B shows the lowest energy configuration obtained from the scans using the B3LYP functional, the water molecule in this case bridges the two diazacrown oxygen atoms.

Table 1 shows the relative energies for both configurations after geometry optimizations with the two density functionals, MP2 and the force field. It can be noticed that the different configurations have energies within 2 kcal/mol of each other for every method. ωb97xd and MP2 both show that configuration A has a lower energy than configuration B yet B3LYP and the force field show the opposite trend.

Similar "bridging " hydrogen bonding between a water molecule and crown oxygen atoms have been reported by Schurhammer *et al*. for crown ethers with a water molecule using QM methods [33]. The lowest energy configuration (by B3LYP/6-311G++(3df,3pd) was one where the D3d structure of 12-crwon-6 was bridged by a water molecule.

Conformation of diazacrown-Na^+-water system

The energy profiles of the scans of the diazacrown-Na^+-water system (Figure 8d) are similar to those of the diazacrown-Na^+ system, where there is a steep well caused by the restriction of the diazacrown conformation by the interaction of the diazacrown with the Na^+. The energetic profile of the scans, however, is complicated by the addition of water molecules, which affect the energy as they interact differently with the diazacrown as the diazacrown conformation changes. There is a lowering of energy for both conformations 1 and 3 (Figure **8**b), compared with conformation 2 (Figure **8**a). Figure S4 shows that conformation 1 and 3 are qualitatively similar and so conformation 3 is shown only in Figure **8**b. In both cases, both water molecules sit with their oxygen atoms interacting with the Na^+. For conformation 2, both water molecules interact with the diazacrown by hydrogen bonding with one of their hydrogen atoms to diazacrown oxygen atoms (water O). For conformations 1 and 3, however, one of the water molecules is able to hydrogen bond to both a diazacrown oxygen atom and a nitrogen atom (water O-N) and this extra hydrogen bonding interaction significantly lowers its energy.

Reorganization/Preorganization of diazacrown

The question regarding the reorganization of the diazacrown upon complexation by Na^+ can addressed by taking the configurations of the diazacrown-Na^+, diazacrown-2water and diazacrown-water configurations and removing the Na^+ or water molecules to leave the diazacrown only. When single-point energies are performed, this provides a measure of the amount of reorganization that must occur for the diazacrown to be complexed by Na^+. Table 2 shows the relative energies, using ωb97xd of the diazacrown configurations where the diazacrown obtained from removing the Na^+ from the diazacrown-Na^+ cluster is set as the reference. Also included are the root mean square displacements (RMSD) between the diazacrown-Na^+ cluster (Na^+ removed) and the other diazacrown conformations. The energy of the lowest-energy diazacrown configuration is -17.01 kcal/mol more stable than the reference, the diazacrown-1water (water removed) is slightly lower, followed by the diazcrown obtained from removing both water molecules from the diazacrown-2water cluster. The RMSD values followed the same trend with the diazacrown-2water (two water molecules removed) diazacrown showing the lowest deviation from the reference. These results indicate that the presence of a water molecule pre-organizes the diazacrown for complexation with Na^+. The presence of another water molecule enhances this effect.

Interaction Energies

Interaction energies, at the ωb97XD/6-311+G(d,p), B3LYP/6-311+G(d,p) and MP2/aug-cc-PVTZ levels of theory, between the diazacrown-Na^+, diazacrown-water diazacrown-water-Na^+ molecular pairs are shown in Table 3. These interactions provide us with a measure of the specific interactions that will be important when the diazacrown is part of the hydraphile sodium channel. In all cases the interaction energies were obtained by taking the lowest energy configurations (from the relaxed scans) for each component of the interaction energy calculation. The diazacrown-Na^+-water interaction energy was calculated by subtracting the Na^+ energy and the diazacrown-water energy from the energy of the diazacrown-Na^+-water system. This interaction energy, therefore, provides the interaction between the Na^+ and the rest of the system.

Calculations using the ωb97XD functional

The diazacrown-Na^+ and diazacrown-Na^+-water systems have similar interaction energies. This indicates an equivalence of both situations, where Na^+ is transported through the lipid bilayer in the presence and absence of extra water molecules. The Na^+-water interaction energy is much smaller than the diazacrown-Na^+ interaction. The diazacrown-water interaction is smaller than that of the Na^+-water interaction

Calculations using the B3LYP functional

The results for B3LYP show a different order of interaction energies with the diazacrown-Na^+-water complex showing more negative interaction energy than the diazacrown-Na^+ complex. This shows a different result to ωB97XD and would indicate that it is more stable for Na^+ to be complexed to the diazacrown in the presence of additional water molecules, particularly as it is transported through a lipid bilayer. For both functionals, the diazacrown-Na$^+$-water energies are similar yet the diazacrown-Na$^+$ interactions are less attractive for the B3LYP functional because of the lack of dispersion contribution for B3LYP. The interaction energy for Na$^+$-water interaction energy is calculated to be less favorable using ωB97XD than the B3LYP functional yet the diazacrown-water interaction is more favorable using ωB97XD than the B3LYP functional. This causes a change in the balance between Na$^+$, diazacrown and water molecules in the diazacrown-Na$^+$-water cluster calculated by B3LYP, compared with ωB97XD.

The difference in order, between ωB97XD than B3LYP, is significant since it provides different conclusions; that is, from the B3LYP calculations we would conclude that water molecules are more likely to accompany Na$^+$ through a bilayer when Na$^+$ is complexed to the diazacrown. The ωB97XD calculations, however, suggest that both scenarios are equally likely.

MP2 Calculations

To address the disparity between the ωB97XD and B3LYP calculations, MP2/aug-cc-PVTZ calculations were performed; this level of theory should be sufficiently high to accurately distinguish between these two cases. The MP2 calculations showed that both energies were almost identical and, in that aspect, agreed with the ωB97XD results. The MP2 energies, however, are less negative by approximately 10 kcal/mol and this could indicate that the dispersion used in the ωB97XD function is overestimated.

The other MP2 energies, diazacrown-water and Na$^+$-water energies were also more similar to the ωB97XD than to the B3LYP energies. The MP2/aug-cc-PVTZ interaction energy was insensitive to small differences in geometry since single-point energies started from the B3LYP, ωB97XD and MP2(6-311G+(d,p)) geometry-optimized structures yielded very similar interaction energies (results not shown).

Force field calculations

The diazacrown-Na$^+$ interaction energy is intermediate between the MP2 and ωB97XD energies but importantly, the diazacrown-Na$^+$-water energy is far greater. One reason for this is because the interaction between Na$^+$ and water is greater than all QM results, which causes more negative interaction energy for the diazacrown-Na$^+$-water cluster.

Comparison of Binding energies with earlier work

Interaction energies can be compared with earlier results for binding energies of Na$^+$ with crown ethers. In the paper by Al-Khahtani et al[24], the binding energy of 18-crown-6 with Na$^+$ was -101.56 kcal/mol (B3LYP, -85.98 kcal/mol diazacrown, this study) and –93.60 kcal/mol (MP2, -80.18 kcal/mol, diazacrown, this study). In the study by De *et al*.[28], it was shown for 18-crown-6, using B3LYP/6-311++G(d,p) that the interaction energy of the most stable cluster was -89.33 kcal/mol. These increased energies indicate the greater binding by diazacrown oxygen atoms than nitrogen atoms.

It was shown by Behjatmanesh-Ardakani[25] that the binding enthalpies of aza-,diaza-, and triaza-12-crown-4 binding with Na$^+$ are lower than our energies (71, 76 and 77 kcal/mol respectively) since there are less binding groups and there was not full complexation because of the smaller cavity. The binding increased with an increasing number of NH groups, which was surprising considering the lower interaction energy in the current study for the diaza-18-crown-6 compared with the 18-crown-6.

Similar Interaction energies were calculated in our earlier work but in that study[67], the interaction energies were not calculated from a rigorous search for the lowest energy configurations. The current work, therefore, provides a significant refinement to that work.

Further Thermodynamic properties

To provide further information regarding the favorability of Na^+ complexation, the enthalpy, entropy and free energy changes are reported for calculations using the DFT with the ωB97XD functional. These values are shown in Table **4**. Also shown are the rotational, translational and vibrational contributions to the entropy. First, dH values are consistently, approximately 2 kcal/mol less negative than the interaction energies. dG values are all less negative than dH values because all dS values are negative (dG=DH-TdS); however, since dS values vary, the differences between dH and dG values also vary. The dS for the diazacrown-water cluster causes the dG to be considerably lower than dH and this causes this interaction free energy to be very small, almost zero. For the diazacrown-water cluster the rotational contribution is the largest. This is because the rotation of water is restricted as a result of interaction with the diazacrown. This rotational entropy may be a key contribution when considering the diazacrown within lipid bilayers since it may offset any interaction the water has with the diazacrown. The vibrational contribution for the diazacrown-water cluster is positive, however, since there are more vibrational degrees of freedom available (hydrogen bonding).

All the translational entropy contributions are similar negative values since there are two molecules interacting to create one molecule. The rotational and vibrational entropy contributions vary considerably, however. For Na^+-water system, there is a positive rotational entropy contribution since the Na^+-water system is less rotationally isotropic than its constituent parts.

The experimental values (mass spectroscopy) [70, 71] for the free energy and enthalpy of the interaction between Na^+ and water are shown in parentheses and match very close to the ωb97xd values.

The effect of implicit Solvation

To gain an understanding of how the diazacrown may behave in bulk water and in the lipid bilayer environments the PCM model was used to calculate the interaction energies of the clusters (Table 6) and relative energies of the diazacrown configurations (Table 5). This was performed with the water solvent and the octane solvent, the octane solvent being used to simulate the hydrophobic environment within a lipid bilayer. First, Table 5 shows relative interaction energies of different conformations of the diazacrown calculated with PCM solvation. For water solvation, there is a very small energy difference between the three configurations. This indicates that within bulk water, the diazacrown should be able to adopt many different configurations. For the octane solvation, there is only a slight difference in relative energies compared with gas phase. This indicates that when the diazacrown is within lower dielectric systems like the lipid bilayer, the conformational behavior should be different. These claims will be tested in future publications in classical molecular dynamics studies.

Table 6 shows the interaction energies of the molecule pairs shown in the PCM solvation models using water and octane. In the presence of the water solvent the interaction energies are much less negative. The effect of the solvation with octane is intermediate between water solvation and gas-phase. In bulk water the complexation is less favored than within a hydrophobic environment. Na^+ can more easily be released from the diazacrown in water but it becomes more stable within a low dielectric environment like the lipid bilayer.

Interestingly, for both water and octane solvation, there is now a difference in the diazacrown-Na^+ and diazacrown-Na^+-water energies. In both cases the diazacrown-Na^+ interaction energy is less negative than the diazacrown-Na^+-water interaction energy; the difference is 8.51 kcal/mol for water solvation and 2.82 kcal/mol for octane solvation. For the water solvation, this may be irrelevant since we are combining explicit and implicit solvation of water. For octane solvation, however, this may be important since it highlights a slight energetic difference between the two different situations and therefore, a preference for the Na^+ to move through a more hydrophobic environment like a lipid bilayer without additional water molecules.

Intermolecular Distances

Selected distances, calculated using DFT with the ωB97XD functional, between molecules in the optimized clusters are shown in Table 7 (diazacrown-water, diazacrown-Na^+ and Na^+-water systems) and Table 8 (the two configurations of the diazacrown-Na^+-water cluster).

For both diazacrown-Na^+ (Table 7) and diazacrown-Na^+-water (Table 8) clusters, Na^+-diazacrown oxygen atom interactions (Na^+-O_{crown} (Direct)) have shorter distances than Na^+-diazacrown nitrogen atom distances (Na^+-N_{crown}(Direct)) indicating that the oxygen atoms are more important for sodium binding than the diazacrown nitrogen atoms.

Force field calculations show that the diazacrown nitrogen atom to Na^+ distances are increased (by 0.14 Å) and diazacrown oxygen atom to Na^+ distance decreased (by 0.05 Å) compared to QM results. In our previous work [67], the radial distribution function (RDF) of Na^+ to diazacrown oxygen and nitrogen atoms, as Na^+ was pulled through a DMPC lipid bilayer, whilst complexed with the terminal diazacrown of the hydraphile, was reported. It showed that the Na^+ to diazacrown oxygen distance centered at 2.3 Å (ranging from 2-2.7 Å) but the Na^+ to diazacrown nitrogen atom distance appeared at much greater distances (ranging from 3.6 to 4.6 Å). Although the force field description of the Na^+-N interaction appears slightly too weak, this may not make a huge difference in the real system since the difference in the optimized configuration is small compared to the difference in the optimized structure and average structure obtained in MD.

In the paper by Du *et al.*, it was shown that the B3LYP/6-311++G(d,p) that for the lowest energy configuration, the crown oxygen atom to Na^+ distance varied from 2.40 to 2.49 Å, which is in a similar range to our results.

One question is whether the Na^+-diazacrown oxygen atom and Na^+-diazacrown nitrogen atom lengths change as a result of complexation of an additional water molecule on each side of the diazacrown. First, we will consider Configuration 2 (see Figure 8, left panel). After the addition of water molecules, there are now two pairs of oxygen atoms (“Water-mediated” and “Direct”, indicated by circles in Figure 8A) with different distances to Na^+. The Na^+-oxygen distances for “Water-mediated” are longer (by 0.78 Å) than those of “Direct” water molecules and this is caused by the involvement of the water molecules; in fact, the water molecules bridge the Na^+-diazacrown oxygen atoms in this case, maintaining a water mediated interaction.

For Configuration 3, there are "Water-mediated" and "Direct" Na^+-diazacrown oxygen interactions but also "Water-mediated" and "Direct" Na^+-diazacrown nitrogen atom interactions. The "Direct" Na^+-O_{crown} distance is smaller than the "water-mediated" distance by 1.13 Å, the "Direct" Na^+-N_{crown} distance is smaller than the "water-mediated" distance by 1.07 Å.

It should be noticed that for both Configuration 2 and 3, the "Direct" interaction distance of the diazacrown-Na^+-water cluster is shorter (by 0.06 Å, Configuration 2, and 0.1 Å, Configuration 3) than the Na^+ to diazacrown oxygen atom distance of the diazacrown-Na^+ cluster. For configuration 2, the Na^+-N_{crown} distance is greater (by 0.11 Å) than for the diazacrown-Na^+ cluster but for Configuration 3, the "direct" Na^+-N_{crown} distance is smaller than the diazacrown-Na^+ cluster by 0.19 Å. The reason for this decreasing of "Direct" distances is because in the diazacrown-Na^+ cluster, the diazacrown oxygen and nitrogen atoms are all competing for Na^+ but when water in mediating, the Na^+ is being pushed towards the "direct" oxygen and nitrogen binders.

The Na^+-water oxygen atom distances for the diazacrown-Na^+-water system are greater than for the equivalent value for the Na^+-water system (2.30-2.36 Å for diazacrown-complexed and 2.35 Å for Na^+-water system). This is because of a lowering of electrostatic interactions when Na^+ is complexed (see NBO analysis below).

In the MD simulations in our previous work, the RDF between the two diazacrown nitrogen atoms of the terminal diazacrown of the hydraphile as Na^+ was pulled through a DMPC lipid bilayer (Shown in Figure S6 in the Supplementary Material). The peak distance is at 8.4 Å but Figure 3b shows that the lowest energy distance is at 5.3 Å for the diazacrown-Na^+ system and Figure 3d shows that the lowest energy distance is at 6 Å for the diazacrown-Na^+-water system. These differences could either be because of discrepancies between the force field and DFT results or because of the effect of condensed phase properties. In future MD studies we will investigate the conformational properties and force field effects of the diazacrown to answer these questions.

The hydrogen bonding distances between water hydrogen atoms with diazacrown oxygen and nitrogen atoms are revealing (see diazacrown/water clusters in Figure 7. The water hydrogen bond distance to the diazacrown oxygen atom is shorter in cluster B than the water hydrogen bond distance to the nitrogen atom was in cluster A, indicating a stronger interaction hydrogen bonding to diazacrown oxygen atoms than to diazacrown nitrogen atoms; this shows a similarity to the Na^+-diazacrown interactions, where interactions to the diazacrown oxygen atoms are shorter than those to nitrogen atoms. One reason is that diazacrown oxygen atoms are more negativley charged than nitrogen atoms causing a greater electrostatic attraction (see section on “NBO analysis” below).

In the parentheses in Table 7 and 8 are the distances for the calculations using the PCM solvation with the water solvent, using DFT with the ωB97XD functional. See the

Supplementary information for related discussion (Section named “**Effect of Solvation model on intermolecular distances”**)

Natural bond orbital analysis

NBO analysis was performed on all the clusters using the ωB97XD functional. NBO analysis provides information about the charges on each atom within a molecule which can lend insight into the strengths of electrostatic interactions and inter/intra-molecular charge transfer and polarization.

The atomic charges are shown in Table 9. Where there is more than one of a particular atom type, the average of the values for the charges are reported. First, the charges for the diazacrown oxygen atoms are more negatively charged than the nitrogen atoms and this explains the greater electrostatic interaction and closer distances to Na^+ and water (seeTable 7 and 8). Furthermore, the water hydrogen to diazacrown oxygen distances are shorter when the diazacrown is complexed to Na^+ (as part of diazacrown-Na^+-water cluster) than the corresponding hydrogen bond distance to the uncomplexed diazacrown. The reason for this can now be explained by the difference in charge of the diazacrown oxygen atoms when complexed by Na^+. Since the diazacrown oxygen atoms become more negatively charged in the presence of Na^+, the interaction with the water hydrogen atom is stronger and this causes a shorter hydrogen bond distance.

Electron transfer within the diazacrown-Na$^+$-water and diazacrown-Na$^+$ clusters

One aspect that should be highlighted, since it should have a large influence on the behavior of the hydraphile-facilitated transport of Na$^+$, is the charge transfer within the diazacrown-Na$^+$-water and diazacrown-Na$^+$ systems. Charge transfer can be monitored with reference to the atom charges and second order pertubation theory.

The charges in Table 9 show that both nitrogen and oxygen atoms are less negatively charged in the free diazacrown compared to the diazacrown complexed with Na$^+$, in the absence and presence of additional water molecules. Furthermore, free Na$^+$ has a charge of +1 but when the Na$^+$ is complexed within the diazacrown the charge is less positive. This implies transfer of electron density from the diazacrown to the Na$^+$; however, the diazacrown oxygen and nitrogen atoms are actually more negatively charged when complexed to the diazacrown. The charges of the hydrocarbon groups, and in particular the hydrogen atoms, are more negative in the complexed diazacrown; that is, there is an inductive affect caused by Na$^+$, where electron density is transferred from the hydrocarbon groups and leaves the oxygen and nitrogen atoms more negatively charged. The presence of extra water molecules, in Configuration 2 of diazacrown-Na$^+$-water cluster, actually reduces the Na$^+$ charge to +0.63 compared to a Na$^+$ charge of +0.68 when it is complexed to the diazacrown with no additional water molecules. This reduction, however, should not purely be because of charge transfer to the water molecules since the Na$^+$ charge is only slighly reduced by the interaction of a water molecule in the Na$^+$-water cluster. Interestingly, the diazacrown oxygen atoms that are farther away from Na$^+$ (“water-mediated”) have a similar charge to “Direct” diazacrown oxygen atoms; this is because they are still connected to the Na$^+$ via the water molecules, a water-mediated electron transfer mechanism (see below). For Configuration 3 of the diazacrown-Na$^+$-water cluster, the charge of Na$^+$ is similar to the Na$^+$ of the diazacrown-Na$^+$ cluster.

The NBO charges for Na$^+$ were also calculated using the solvation model and these are shown in the parentheses of Table 5. It can be noticed that the charges are not affected significantly by the solvation model.

Even though electron density originates from the hydrocarbon groups, during the complexation of Na$^+$, electron transfer from the oxygen and nitrogen atoms to the Na$^+$ should be dominant. This is confirmed by second order-perturbation theory, which tests whether there is an electron donation from one atom to another. This electron donation results in a stabilization and the energy of stabilization is given by

$$\Delta \boldsymbol{E_{ij}} = \frac{\boldsymbol{q_i F(i,j)^2}}{\boldsymbol{\epsilon_j - \epsilon_i}}$$

where q_{i} is the donor orbital occupancy, ε_{i} and ε_{j} are orbital energies and F(i,j) is the off-diagonal NBO Fock matrix element. For the diazacrown-Na$^+$ cluster, the largest stabilizations are given by donations from diazacrown oxygen and nitrogen lone pairs (13.41 and 7.84 kcal/mol respectively) to sodium lone pair orbitals.

For the diazacrown-Na$^+$-water cluster, the water bridging charge transfer between diazacrown oxygen atoms (Direct) and Na$^+$ should be shown in second-order pertubation theory. First, for Configuration 2, there is electron density donation from the water molecules to Na$^+$, but not for the water-Na$^+$ cluster, indicating the donation is not inherent to water-Na$^+$ interactions. The donation is shown by large stabilizations from “water-mediated” diazacrown oxygen atoms to the water molecules (diazacrown oxygen lone pairs to water oxygen-hydrogen antibonding orbitals – largest stabilization is 6.75 kcal/mol). Moreover, there is electron density donation from bridging water oxygen lone pairs and from hydrogen-oxygen bonding orbitals (largest is 10.28 and 8.08 kcal/mol, respectively) to Na$^+$ lone pairs. Moreover, there is water-mediated electron transfer from the diazacrown oxygen to Na$^+$.

For configuration 3, there is a similar water-mediated electron transfer mechanism (see section named “**Water mediated charge-transfer for Configuration 3 of diazacrown-Na$^+$-water cluster”** in the Supplementary material).

We can now provide a description of charge transfer that occurs from the diazacrown to Na$^+$ and this is represented in Figure 9, where arrows show the direction of electron transfer. There are two mechanisms for electron transfer from the diazacrown. For mechanism 1 there is electron transfer from the diazacrown hydrocarbon groups to the diazacrown oxygen and nitrogen atoms followed by direct electron transfer from diazacrown oxygen and nitrogen atoms to Na$^+$. Conversely, in Mechanism 2 there is water-mediated electron transfer where there is electron transfer from “Water-mediated” diazacrown oxygen atoms to the water molecule followed by electron transfer from the water molecule to the Na$^+$. In this case there is also the initial electron density transfer from the diazacrown hydrocarbon groups to the diazacrown oxygen and nitrogen atoms. This is evidenced by the increase in positive charge of the hydrocarbon hydrogen atoms for the Na^+ complexed (+0.19) clusters compared to the diazacrown-only cluster (+0.17).

The overall effects of the electron transfer mechanisms makes the Na^+ less negatively charged, which should make Na^+ less hydrophilic and more favorable within the lipid bilayer. This work, therefore, highlights a tactic for the design of better sodium channels, namely to increase this electron transfer further to reduce the effective charge of Na^+[32]. This tactic may not only be used for the development of ion channels but for other applications, where it would be beneficial for the complexing of metal ions to be improved, such as the removal of metal ions from nuclear waste[72].

Implications of results for action of hydraphile sodium channel

Previous experimental data only provides information about transfer rates of Na^+ of various hydraphiles with different substituents [14, 20] but has yet to be able to probe the detailed molecular and electronic aspects of the process. The present paper investigates the coordination of Na^+ with the diazacrown moieties of the hydraphiles and provides insight into this process in the following ways:

1) The interaction energy of Na^+ with the diazacrown and water molecules is similar to that of the diazacrown in the presence of additional water molecules (for ωB97XD and MP2/aug-cc-PVTZ calculations); the interaction energy result offer an explanation for the effectiveness of the hydraphile. Since the interaction energies are similar it is likely that both mechanisms are possible (Na^+ in the presence and absence of water molecules). Our previous work suggested that when the number of solvent states

increases, there are a greater number of mechanisms that are available for transport of Na^+ and this could mean that the transport process is more likely [67].

2) There is hydrogen bonding between the diazacrown oxygen and nitrogen atoms and water and this may be responsible for water ordering and channel forming in the hydraphile as proposed by Murray *et al.*[22]. The presence of Na^+ within the diazacrown actually strengthens the water diazacrown interaction and this may be a factor in the ordering of water. The ordering of water molecules and reduction of rotational entropy may offset this effect, however. We are currently working molecular dynamics simulations, investigating how the hydraphile can stabilize a water channel.
3) It is likely that charge transport is a key factor in the facilitated transport of Na^+ by the hydraphile since it will make it less charged and more ready to pass through the hydrophobic lipid bilayer. The presence of water molecules accompanying the Na^+ with the diazacrown actually increase the charge transfer via a water mediated mechanism and may increase this effect.

The accuracy of QM method and force field

This study highlights how important density functional choice is when considering the interaction between ions, diazacrowns and water molecules. Whereas calculations using the B3LYP functional predicted the sodium cation to be more favorable within the diazacrown, in the presence of additional water molecules rather than in their absence, calculations using the ωB97XD functional showed that both interactions were similar. This was confirmed by MP2/aug-cc-PVTZ calculations. The force field calculation shows an even greater difference in interaction energies between the two systems and this could have profound effects when it comes to simulating the transport of Na^+ through the lipid bilayer. It should be noted that the Na^+-water interaction, which drives the difference in interaction energy for the force field involves electrostatic and Lennard-Jones parameters of a well-established force field (TIP3P water[73] and ion FF of Beglov and Roux[73]). Modifying these parameters could modify the condensed phase properties of ion solvation or the dizacrown-Na^+ interaction. Moreover, the NBO analysis has shown that the diazacrown causes a significant decrease in the charge of the Na^+, which would in-turn cause a decrease in the water-Na^+ interactions and this strongly points to the necessity of polarization when considering the interaction of Na^+ within the diazacrown; this is even more important than when Na^+ is solvated in bulk water. There is already a polarized force field, which can treat lipid bilayers[74, 75]. The work here suggests that for accurate classical simulations, which will capture the hydraphile-assisted transport behavior and thermodynamics, a polarizable force field for the diazacrown will need to be parameterized and adopted.

We showed results of the diazacrown with implicit solvent in octane and water to provide information regarding how a change in environment may affect the results; however, to gain further understanding of the detailed behavior of the diazacrown in lipid bilayer, we should gain an understanding of the interaction of explicit lipid molecules with the diazacrown and such a study is currently being conducted within our group.

Conclusions

The results of the present study have helped to highlight the factors that affect how Na^+ is transported through a lipid bilayer by an artificial sodium channel, the hydraphile. Quantum chemical calculations (DFT, using two different functional, and MP2 calculations) of a fragment of the hydraphile, the diazacrown, were performed to provide detailed information about the complexation of Na^+. This study follows on from our previous study that investigated the mechanism of the hydraphile within a lipid bilayer using classical molecular dynamics. In the present study, the QM calculations were, therefore, used to, both, scrutinize the accuracy of the force field, improve the force used and provide greater detail, including the electronic structure that force field methods cannot provide.

Calculations of water interactions with Na^+ and of water interactions with the diazacrown were calculated for comparison. There is electron donation from the hydrocarbon groups of the diazacrown to the diazacrown oxygen and nitrogen atoms, which then donate electron density to the Na^+, diminishing the positive charge of Na^+. When extra water molecules are added to the diazacrown-Na^+ system, the water hydrogen atoms became hydrogen-bonded with the diazacrown oxygen atoms, bridging the diazacrown oxygen-Na^+ interaction. The water molecules could then mediate the electron transfer from the diazacrown oxygen atom to the Na^+.

Results attained at the highest level of theory (MP2/aug-cc-PVTZ) agree with results of DFT with the ωB97XD functional that the interaction energy of Na^+ with the diazacrown is the same value as in the presence of extra water molecules and this could be key to the success of the hydraphile Na^+ channel. It was shown that water molecules interact with the diazacrown by hydrogen bonding to two oxygen atoms and bridging to another oxygen or nitrogen atom and water molecules help to pre-organize the diazacrown ready to accept the sodium ions. Moreover, it is thought that the hydraphile reorganizes water within a lipid bilayer and rotational entropy losses upon interaction of water molecules with the diazacrown may weaken this interaction and be important when considering this process.

The present study shows how important density functional choice is when considering the delicate balances between water, Na^+ and ion-complexing molecules. Density functionals that correctly treat dispersion interactions should be more effective in this respect. This was confirmed by MP2/aug-cc-PVTZ calculations.

Overall, this study provides a a detailed molecular, energetic and electronic basis for the different interactions involved within the diazacrown functional groups of hydraphile sodium channels, was provided; this understanding takes us a step closer to providing a comprehensive description of the mechanism of action of the hydraphile sodium channel and will help in designing more effective sodium channels in the future.

Acknowledgments

We would like to thank the Centre for High Performance Computing (CHPC) in Cape Town, South Africa for computing resources.

Tables

Table 1: Relative energies (in Kcal/mol) of three different structures of the diazacrown

		B3LYP	ωb97xd	MP2	FF
diazacrown	D_{3d}	3.86	8.95 (5.81)	7.35	9.09
	C_i	0.75	0	0	0
	Mixed	0	2.21 (0.87)	2.13	3.093
diazacrown-water	A	1.27	0	0	1.71
	B	0	0.87	0.93	0
diazacrown-water-Na^+	2	1.73	1.85 (0.30)	1.60	0
	3	0	0	0	0.34

Table 2: Relative energies and root-mean-square deviations of diazacrown conformations after reorganization. Zero is set by the energy of the diazacrown after the Na^+ was removed from the diazacrown-Na^+ cluster.

Cluster	Relative energy (kcal/mol)	RMSD (Å)
diazacrown-Na^+	0	0
diazacrown	-17.01	1.47
diazacrown- 1 water	-10.27	1.19
diazacrown – 2 water	-5.42	0.78

Table 3 : Interaction energies of the molecule pairs shown in Figures 4-7. All energies are in Kcal/mol. A) and B) indicate the different configurations shown in Figure 7.

	B3LYP/6-311G+(d,p) (kcal/mol)	ωb97xd/ 6-311G+(d,p) (kcal/mol)	MP2/ aug-cc-PVTZ (kcal/mol)	Force field (kcal/mol)
diazacrown-water	-8.002	-14.21	-13.28	-5.14
diazacrown-Na^+	-85.98	-91.52	-80.18	-86.09
diazacrown-Na^+-water	-90.29	-90.51	-80.67	-103.97
Na^+-water	-25.78	-24.76	-22.36	-29.73

Table 4 : Enthalpy, Entropy and free energy changes of the molecule pairs shown in Figures 4-7. Also included are the individual contributions, translational (Trans), rotational (Rot) and vibrational (Vib), of the entropy.

	dH (kcal/mol)	dG (kcal/mol)	dS cal/mol/K	Rot cal/mol/K	Trans cal/mol/K	Vib cal/mol/K
diazacrown-water	-12.15	-1.66	-35.20	-10.03	-34.43	9.53
diazacrown-Na^+	-88.96	-79.95	-30.24	-0.03	-35.11	4.90
diazacrown-Na^+-water	-89.38	-81.85	-25.27	0.142	-35.13	9.72
Na^+-water	-23.76 (24.00[70, 71])	-17.22 (17.59[70, 71])	-21.96	7.86	-32.88	3.06

Parentheses show experimental results with citations

Table 5: Relative interaction energies of different conformations of diazacrown using PCM solvation model with water and octane

	No solvation (kcal/mol)	Water (kcal/mol)	Octane (kcal/mol)
D_{3d}	8.95	0.063	7.81
C_i	0	0	0
Mixed	2.21	0.63	2.13

Table 6 : Interaction energies of the molecule pairs in this study with the PCM solvation models using water and octane. All energies are in Kcal/mol.

	Solvation (water)	Solvation (octane)
diazacrown-water	-11.88	-13.02
diazacrown-Na^+	-23.05	-58.09
diazacrown-Na^+-water	-14.54	-55.27
Na^+-water	-3.17	-13.74

Table 7 : Selected distances within diazacrown-water, diazacrown-Na+ and water-Na+ clusters. The 6-311G+(d,p) basis set was used for all geometry optimization calculations. Parentheses show distances calculated using the PCM water solvation model.

System	Interaction	Distance (Å) (ωB97XD)	Distance (Å) (FF)
diazacrown-water	H_{water}-N_{crown} (A)	2.14	2.24
	H_{water}-O_{crown} (A)	--	2.02
	H_{water}-N_{crown} (B)	--	--
	H_{water}-O_{crown}(B)	1.94	2.02
diazacrown-Na^+	Na^+-O_{crown}	2.50 (2.55)	2.45
	Na^+-N_{crown}	2.69 (2.59)	2.83
Na^+- water	Na^+-O_{water}	2.25 (2.37)	2.21

Table 8: Selected distances within diazacrown-Na^+-water clusters

diazacrown-Na^+-Water Configuration 2	Interaction	ωb97XD Length (Å)	FF Length (Å)
	$H_{water\ O}$-O_{crown}	1.84 (1.82)	1.96
	Na^+-O_{crown} (Direct)	2.44 (2.47)	2.38
	Na^+-O_{crown} (Water-mediated)	3.22 (3.21)	3.36
	Na^+-N_{crown} (Direct)	2.80 (2.81)	3.60
	Na^+-$O_{water\ O}$	2.36 (2.41)	2.25
diazacrown-Na^+-water Configuration 3	$H_{water\ O}$-O_{crown}	1.79 (1.80)	1.9
	$H_{water\ O\text{-}N}$-O_{crown}	1.95 (1.85)	2.07
	$H_{water\ O\text{-}N}$-N_{crown}	1.97 (1.96)	2.19
	Na^+-O_{crown} (Direct)	2.40 (2.42)	2.37
	Na^+-O_{crown} (Water mediated)	3.53 (3.77)	3.50
	Na^+-N_{crown} (Direct)	2.52 (2.56)	2.52
	Na^+-N_{crown} (Water mediated)	3.59 (3.67)	3.75
	Na^+-$O_{water\ O\text{-}N}$	2.34 (2.45)	2.24
	Na^+-$O_{water\ O}$	2.30 (2.36)	2.23

Table 9: NBO charges (in elementary charge units, e) for different atom groups within the Clusters, calculated with DFT using the ωB97XD functional.

	O_{crown}	N_{crown}	Na^+	O_{wat}	H_{crown}
diazacrown-Na^+-Water 2	-0.62	-0.58	0.63 (0.64)	-0.96	0.19
diazacrown-Na^+-Water 3	-0.62	-0.59	0.68 (0.72)	-0.978	0.19
diazacrown-Na^+	-0.62	-0.59	0.68 (0.67)	--	0.19
Na^+-1 water	--	--	0.996 (0.998)	-1.01	--
Water	--	--	--	-0.92	--
diazacrown	-0.60	-0.56	--	--	0.17

Parentheses show values from the PCM model with water

Figures

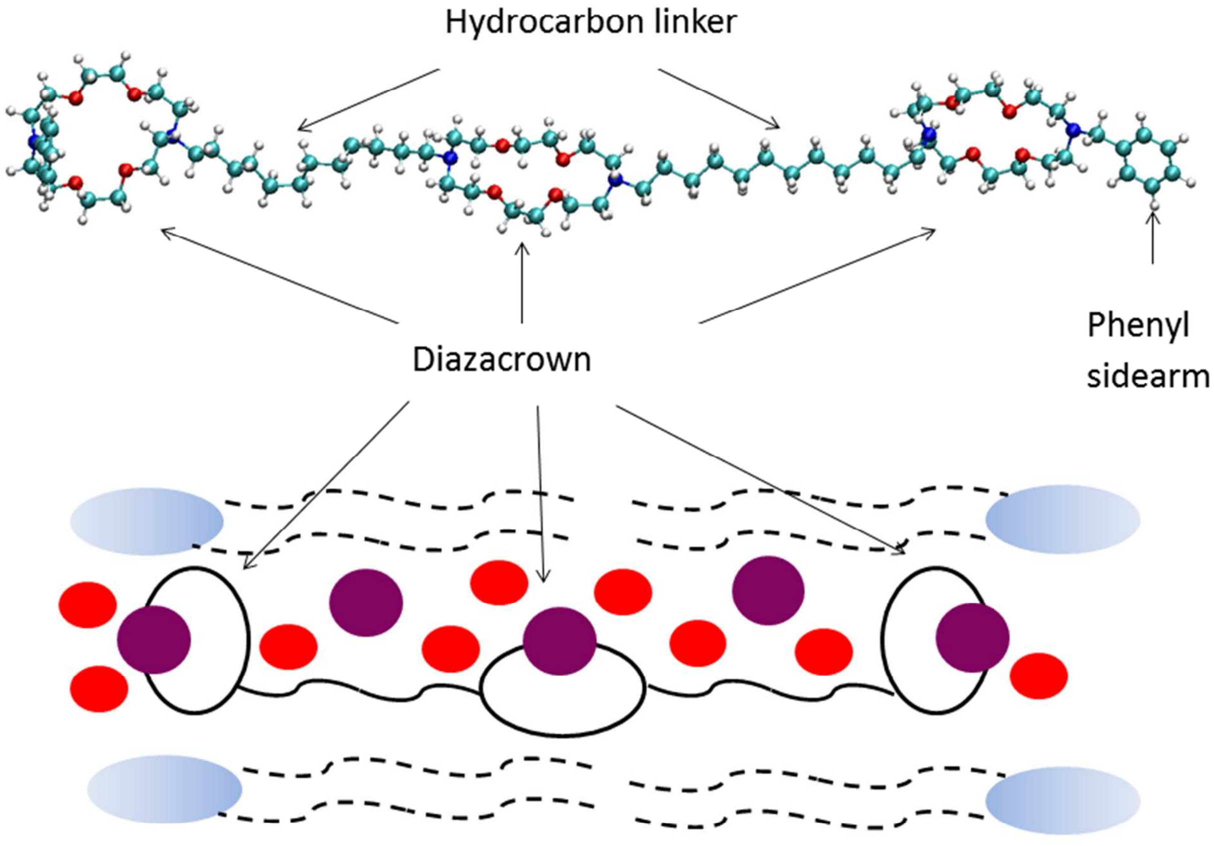

Figure 1 : Top panel shows a simulation model of a typical hydraphile molecule showing three diazacrown molecules connected by hydrocarbon linkages. Bottom panel shows the current model for the action of the hydraphile as a cation transporter within a lipid bilayer. Dotted lines and blue ovals represent lipid molecules. Solid lines are the hydraphile, red spheres are water molecules and purple spheres Na^+ cations. Graphic idea is taken from Gokel and Negin [18]

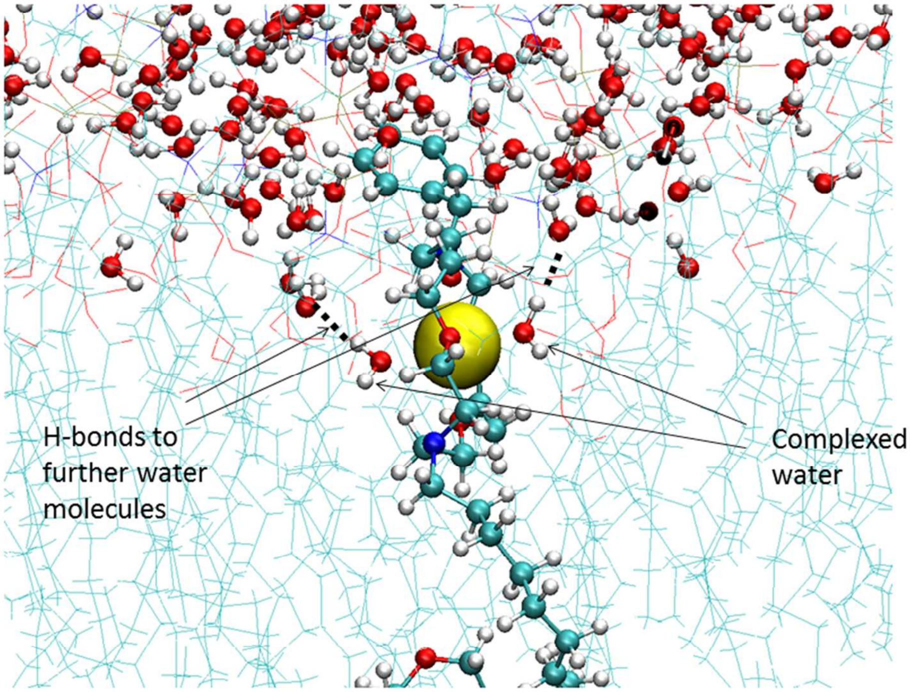

Figure 2: A snapshot from a molecular dynamics simulation of the Na^+ being pulled through a DMPC lipid bilayer whilst complexed with the terminal diazacrown of the hydraphile.

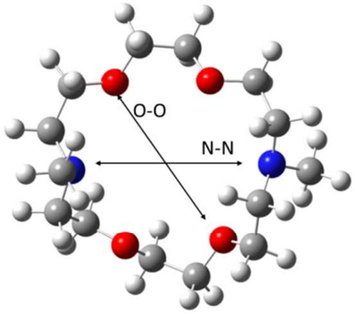

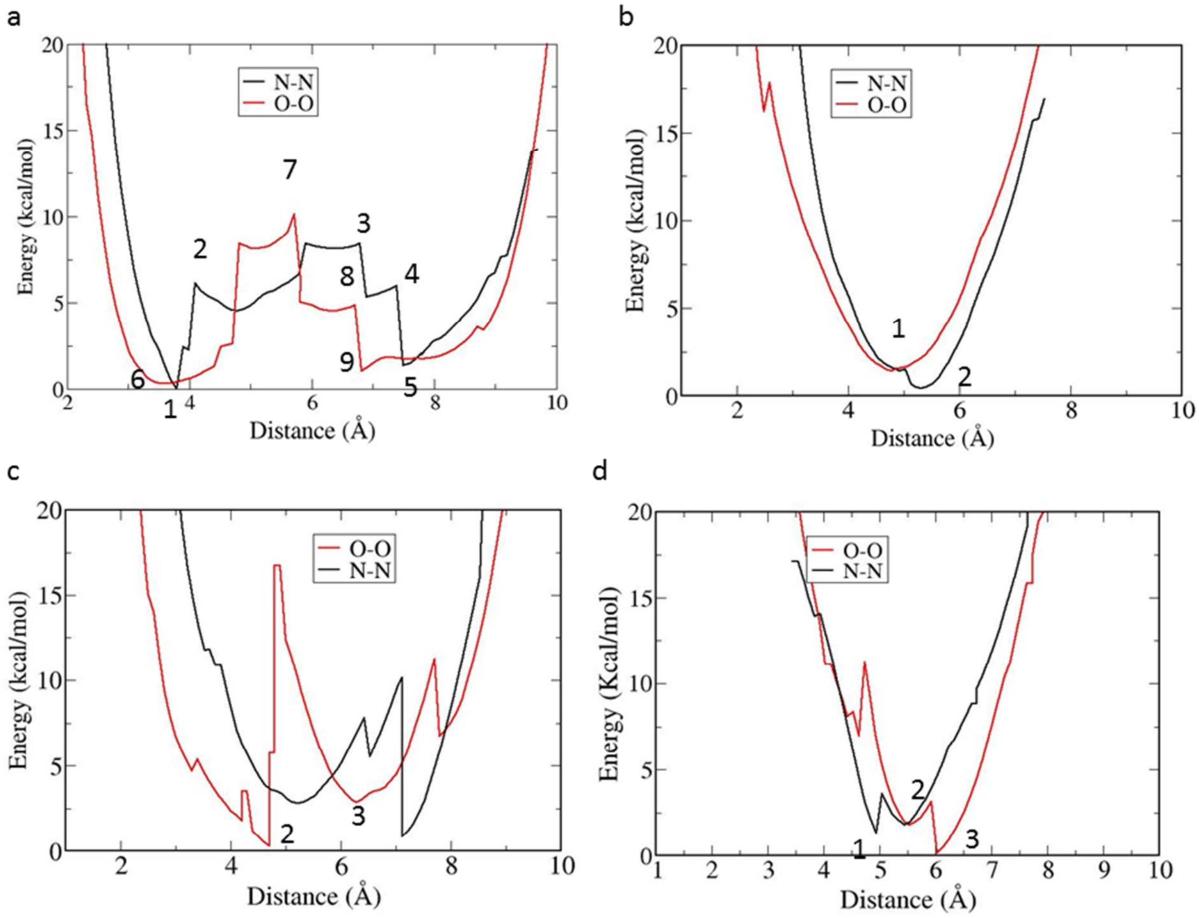

Figure 3: Scans of O-O and N-N distances within the diazacrown for systems containing, a) diazacrown, b) diazacrown-Na^+ c) diazacrown-water d) diazacrown-water-Na^+.

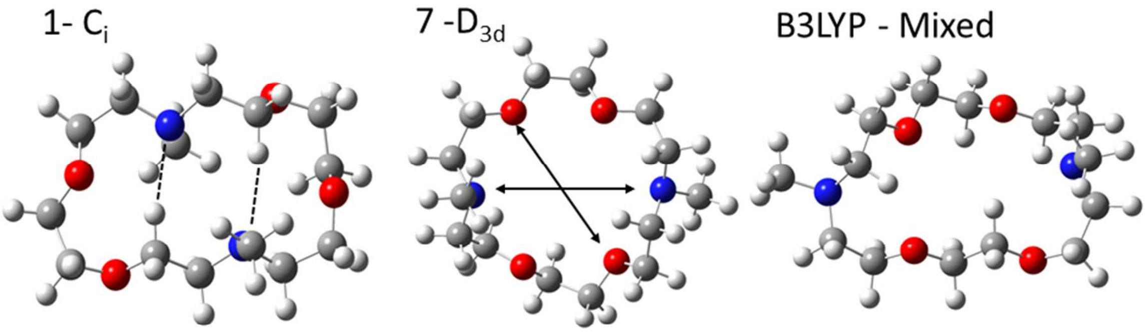

Figure 4: The diazacrown in three different conformations. The numbers relate to numbers is the scans in Figure 3a. Configuration 1 is the lowest energy configuration found in this study. The arrows in b show the distances (N-N and O-O) that were scanned. The right panel shows the lowest energy configuration obtained from the scan using the B3LYP functional.

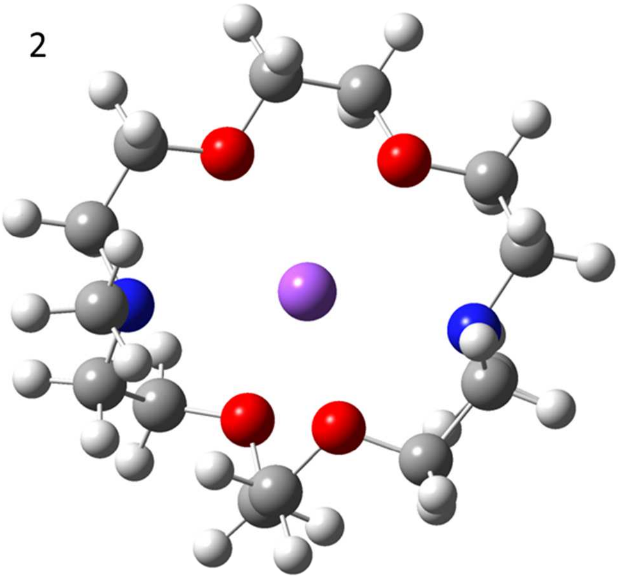

Figure 5: The diazacrown-Na$^+$ system at its minimum energy structure. The number relates to the number shown in Figure 3b - the lowest energy configuration found in this study.

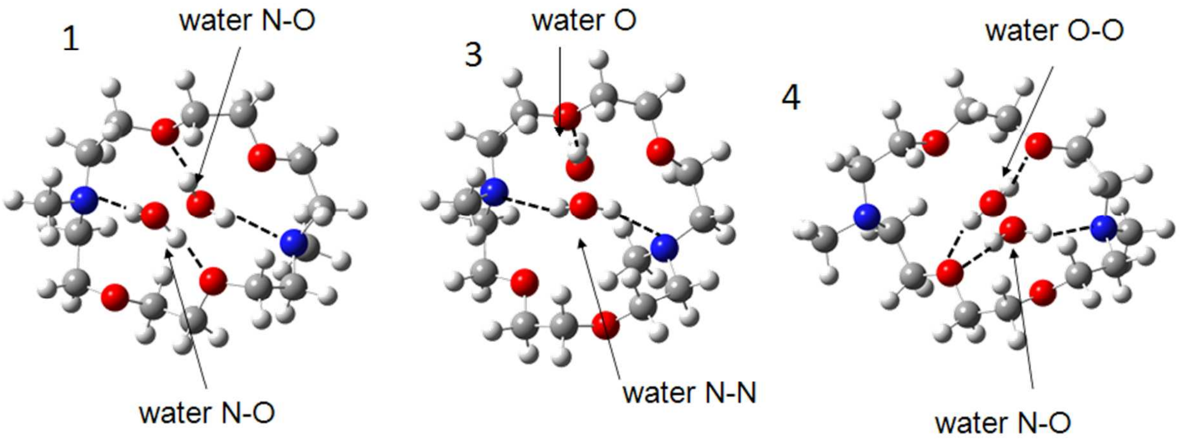

Figure 6: Configurations of the diazacrown-2water system. The numbers relate to numbers is the scans in Figure 3c. Configuration 1 is the lowest energy configuration found in this study. Water N-O refers to a water molecule that is hydrogen bonding with a diazacrown nitrogen and oxygen atom, Water O-O refers to a water molecule that is hydrogen bonding with a two diazacrown oxygen atoms, Water N-N refers to a water molecule that is hydrogen bonding with a two diazacrown nitrogen atoms, Water O refers to a water molecule that is hydrogen bonding with only one diazacrown oxygen atom.

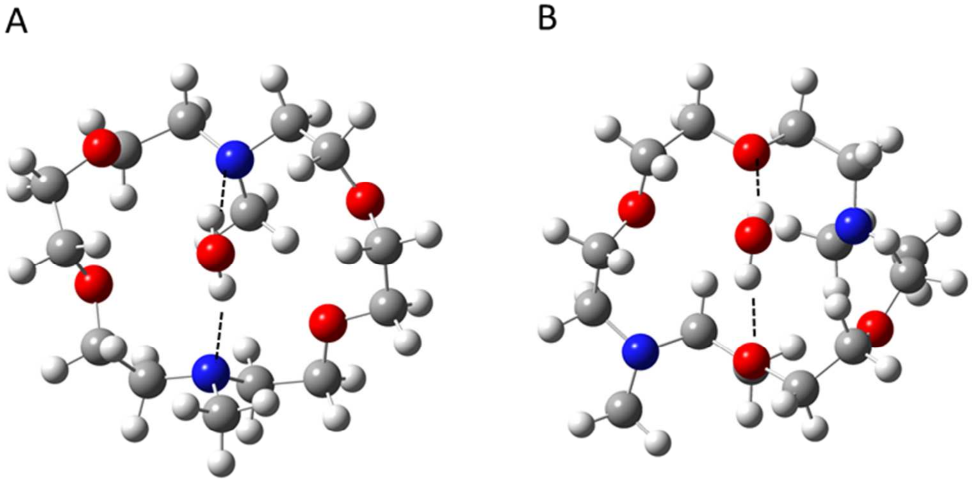

Figure 7. Diazacrown/water clusters. A. A single water molecule is hydrogen bonded with a nitrogen and oxygen atom B. A water molecule is hydrogen bonded with two oxygen atoms and additionally interacts with a nitrogen atom.

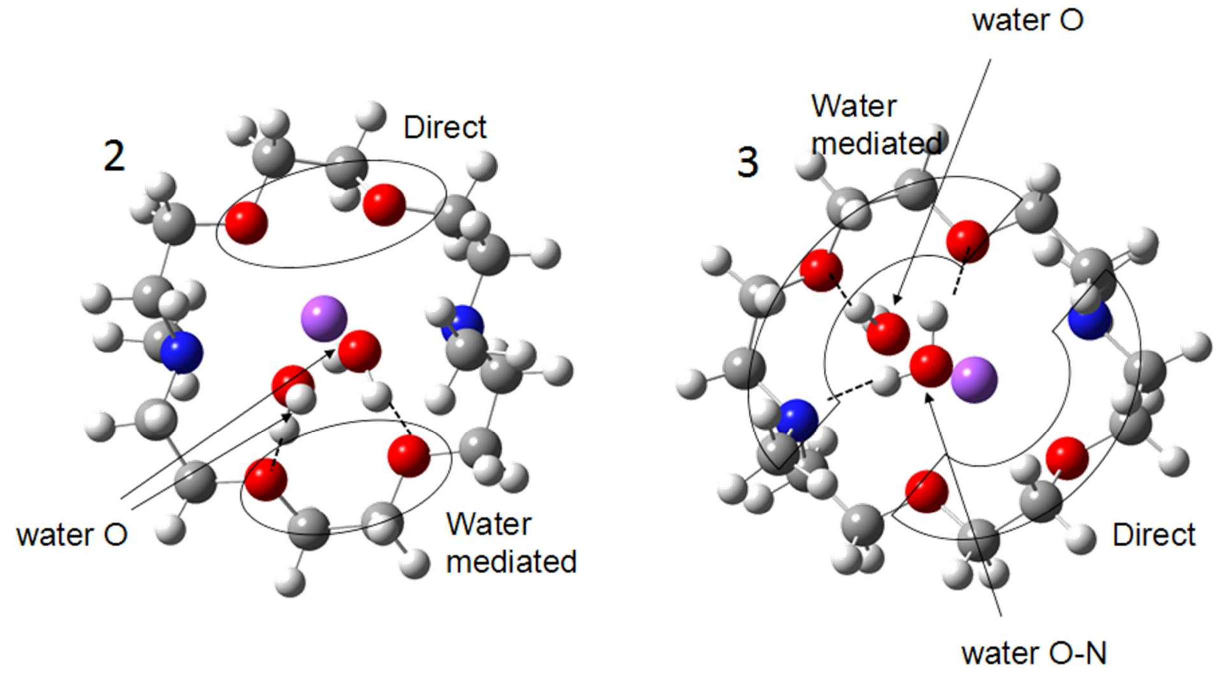

Figure 8: Configurations of the diazacrown-Na$^+$- 2water system. The numbers relate to numbers is the scans in Figure 3c. Configuration 3 is the lowest energy configuration found in this study. Water O refers to a water molecule that is hydrogen bonding with only one diazacrown oxygen atom and Water O-O refers to a water molecule that is hydrogen bonding with a two diazacrown oxygen atoms.

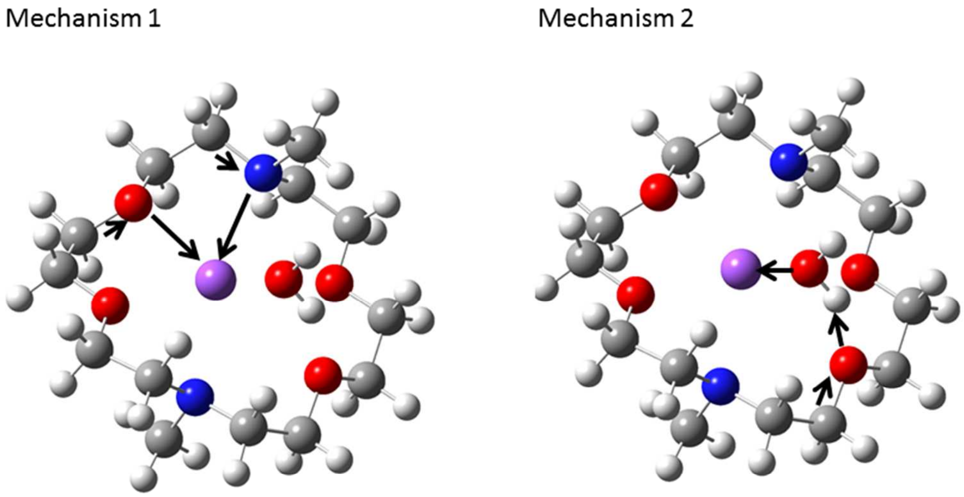

Mechanism 1

Mechanism 2

Figure 9: A representation of the electron transfer shown in NBO calculations. Mechanism 1: There is electron transfer from the hydrocarbon groups to the diazacrown oxygen atoms followed by direct transfer from the diazacrown oxygen and nitrogen atoms to Na^+. Mechanism 2: There is water-mediated electron transfer from diazacrown oxygen atoms to Na^+ (diazacrown oxygen to water hydrogen and water oxygen to Na^+).

References

1. K. S. J. Iqbal and P. J. Cragg, *Dalton Transactions*, 2007, DOI: 10.1039/b613867p, 26-32.
2. D. M. Hutt, C. A. Olsen, C. J. Vickers, D. Herman, M. A. Chalfant, A. Montero, L. J. Leman, R. Burkle, B. E. Maryanoff, W. E. Balch and M. R. Ghadiri, *Acs Medicinal Chemistry Letters*, 2011, **2**, 703-707.
3. P. V. Jog and M. S. Gin, *Organic Letters*, 2008, **10**, 3693-3696.
4. N. Sakai and S. Matile, *Langmuir*, 2013, **29**, 9031-9040.
5. W. M. Leevy, G. M. Donato, R. Ferdani, W. E. Goldman, P. H. Schlesinger and G. W. Gokel, *Journal of the American Chemical Society*, 2002, **124**, 9022-9023.
6. S. McLaughlin and M. Eisenberg, *Annual Review of Biophysics and Bioengineering*, 1975, **4**, 335-366.
7. B. A. Smith, M. M. Daschbach, S. T. Gammon, S. Xiao, S. E. Chapman, C. Hudson, M. Suckow, D. Piwnica-Worms, G. W. Gokel and W. M. Leevy, *Chemical Communications*, 2011, **47**, 7977-7979.
8. J. L. Atkins, M. B. Patel, Z. Cusumano and G. W. Gokel, *Chemical Communications*, 2010, **46**, 8166-8167.
9. W. Wang, C. R. Yamnitz and G. W. Gokel, *Heterocycles*, 2007, **73**, 825-+.
10. G. W. Gokel and S. Negin, *Advanced Drug Delivery Reviews*, 2012, **64**, 784-796.
11. A. Nakano, Q. Xie, J. V. Mallen, L. Echegoyen and G. W. Gokel, *Journal of the American Chemical Society*, 1990, **112**, 1287-1289.
12. G. W. Gokel and A. Mukhopadhyay, *Chemical Society Reviews*, 2001, **30**, 274-286.
13. G. W. Gokel, *Chemical Communications*, 2000, DOI: 10.1039/a903825f, 1-9.
14. M. E. Weber, W. Wang, S. E. Steinhardt, M. R. Gokel, W. M. Leevy and G. W. Gokel, *New Journal of Chemistry*, 2006, **30**, 177-184.
15. H. Shabany, R. Pajewski, E. Abel, A. Mukhopadhyay and G. W. Gokel, *Journal of Heterocyclic Chemistry*, 2001, **38**, 1393-1400.
16. G. W. Gokel and I. A. Carasel, *Chemical Society Reviews*, 2007, **36**, 378-389.
17. G. W. Gokel and M. M. Daschbach, *Coordination Chemistry Reviews*, 2008, **252**, 886-902.
18. G. W. Gokel and S. Negin, *Accounts Chem. Res.*, 2013, **46**, 2824-2833.
19. C. L. Murray and G. W. Gokel, *Chemical* Communications, 1998, DOI: 10.1039/a806317f, 2477-2478.
20. E. Abel, G. E. M. Maguire, O. Murillo, I. Suzuki, S. L. De Wall and G. W. Gokel, *Journal of the American Chemical Society*, 1999, **121**, 9043-9052.
21. H. Shabany, C. L. Murray, C. A. Gloeckner, M. A. Grayson, M. L. Gross and G. W. Gokel, *Chemical Communications*, 2000, DOI: 10.1039/b005442i, 2375-2376.
22. C. L. Murray, H. Shabany and G. W. Gokel, *Chemical Communications*, 2000, DOI: 10.1039/b005431n, 2371-2372.
23. G. Srinivas, C. F. Lopez and M. L. Klein, *Journal of Physical Chemistry B*, 2004, **108**, 4231-4235.
24. A. A. Al-Kahtani, N. A. Al-Jallal and A. A. El-Azhary, *Spectrochimica Acta Part a-Molecular and Biomolecular Spectroscopy*, 2014, **132**, 70-83.
25. R. Behjatmanesh-Ardakani, *Struct. Chem.*, 2014, **25**, 919-929.
26. A. Boda, S. M. Ali, H. Rao and S. K. Ghosh, *J. Mol. Model.*, 2012, **18**, 3507-3522.
27. A. D. Bokare and A. Patnaik, *Journal of Physical Chemistry A*, 2005, **109**, 1269-1271.
28. S. De, A. Boda and S. M. Ali, *Journal of Molecular Structure-Theochem*, 2010, **941**, 90-101.

29. D. Feller, M. A. Thompson and R. A. Kendall, *Journal of Physical Chemistry A*, 1997, **101**, 7292-7298.
30. J. Golebiowski, V. Lamare, M. T. C. Martins-Costa, C. Millot and M. F. Ruiz-Lopez, *Chemical Physics*, 2001, **272**, 47-59.
31. X. J. Guo, Y. D. Zhu, M. J. Wei, X. M. Wu, L. H. Lu and X. H. Lu, *Chin. J. Chem. Eng.*, 2011, **19**, 212-216.
32. S. Hadisaputra, L. R. Canaval, H. D. Pranowo and R. Armunanto, *Mon. Chem.*, 2014, **145**, 737-745.
33. R. Schurhammer, P. Vayssiere and G. Wipff, *Journal of Physical Chemistry A*, 2003, **107**, 11128-11138.
34. M. A. Thompson, *Journal of Physical Chemistry*, 1995, **99**, 4794-4804.
35. M. A. Thompson, *Int. J. Quantum Chem.*, 1996, **60**, 1133-1141.
36. M. A. Thompson, E. D. Glendening and D. Feller, *Journal of Physical Chemistry*, 1994, **98**, 10465-10476.
37. M. Valente, S. F. Sousa, A. L. Magalhaes and C. Freire, *J. Mol. Model.*, 2011, **17**, 3275-3288.
38. P. R. Varadwaj, A. Varadwaj, G. H. Peslherbe and H. M. Marques, *Journal of Physical Chemistry A*, 2011, **115**, 13180-13190.
39. G. Benay and G. Wipff, *Journal of Physical Chemistry B*, 2014, **118**, 13913-13929.
40. L. X. Dang, *Journal of the American Chemical Society*, 1995, **117**, 6954-6960.
41. L. X. Dang and P. A. Kollman, *Journal of Physical Chemistry*, 1995, **99**, 55-58.
42. P. D. J. Grootenhuis and P. A. Kollman, *Journal of the American Chemical Society*, 1989, **111**, 2152-2158.
43. P. D. J. Grootenhuis and P. A. Kollman, *Journal of the American Chemical Society*, 1989, **111**, 4046-4051.
44. T. Kowall and A. Geiger, *Journal of Physical Chemistry*, 1994, **98**, 6216-6224.
45. T. Kowall and A. Geiger, *Journal of Physical Chemistry*, 1995, **99**, 5240-5246.
46. F. T. H. Leuwerink and W. J. Briels, *Journal of Chemical Physics*, 1995, **103**, 4637-4652.
47. F. T. H. Leuwerink, S. Harkema, W. J. Briels and D. Feil, *Journal of Computational Chemistry*, 1993, **14**, 899-906.
48. P. Sahu, S. M. Ali and J. K. Singh, *J. Mol. Model.*, 2014, **20**.
49. T. P. Straatsma and J. A. McCammon, *Journal of Chemical Physics*, 1989, **91**, 3631-3637.
50. Y. X. Sun and P. A. Kollman, *Journal of Computational Chemistry*, 1992, **13**, 33-40.
51. G. Wipff, *J. Coord. Chem.*, 1992, **27**, 7-37.
52. G. Wipff and M. Lauterbach, *Supramol. Chem.*, 1995, **6**, 187-+.
53. D. Zanuy, J. Preat, E. A. Perpete and C. Aleman, *Journal of Physical Chemistry B*, 2012, **116**, 4575-4583.
54. M. C. Zwier, J. W. Kaus and L. T. Chong, *Journal of Chemical Theory and Computation*, 2011, **7**, 1189-1197.
55. M. K. Ghosh, S. Re, M. Feig, Y. Sugita and C. H. Choi, *Journal of Physical Chemistry B*, 2013, **117**, 289-295.
56. B. B. Lev, D. R. Salahub and S. Y. Noskov, *Interdiscip. Sci.*, 2010, **2**, 12-20.
57. S. S. Azam, T. S. Hofer, B. R. Randolf and B. M. Rode, *Journal of Physical Chemistry A*, 2009, **113**, 1827-1834.
58. S. S. Azam, H. Zaheer ul and M. Q. Fatmi, *J. Mol. Liq.*, 2010, **153**, 95-100.
59. C. W. Liu, F. Wang, L. J. Yang, X. Z. Li, W. J. Zheng and Y. Q. Gao, *Journal of Physical Chemistry B*, 2014, **118**, 743-751.
60. G. W. Gokel, W. M. Leevy and M. E. Weber, *Chemical reviews*, 2004, **104**, 2723-2750.
61. J. B. Burkhardt, A. A. Skelton and J. R. Fried, *Soft Matter*, 2013, **9**, 4444-4454.

62. A. D. Becke, *Journal of Chemical Physics*, 1993, **98**, 1372-1377.
63. J. D. Chai and M. Head-Gordon, *Journal of Chemical Physics*, 2008, **128**, 15.
64. M. J. Frisch, G. W. Trucks, H. B. Schlegel, G. E. Scuseria, M. A. Robb, J. R. Cheeseman, G. Scalmani, V. Barone, B. Mennucci, G. A. Petersson, H. Nakatsuji, M. Caricato, X. Li, H. P. Hratchian, A. F. Izmaylov, J. Bloino, G. Zheng, J. L. Sonnenberg, M. Hada, M. Ehara, K. Toyota, R. Fukuda, J. Hasegawa, M. Ishida, T. Nakajima, Y. Honda, O. Kitao, H. Nakai, T. Vreven, J. J. A. Montgomery, J. E. Peralta, F. Ogliaro, M. Bearpark, J. J. Heyd, E. Brothers, K. N. Kudin, V. N. Staroverov, R. Kobayashi, J. Normand, K. Raghavachari, A. Rendell, J. C. Burant, S. S. Iyengar, J. Tomasi, M. Cossi, N. Rega, N. J. Millam, M. Klene, J. E. Knox, J. B. Cross, V. Bakken, C. Adamo, J. Jaramillo, R. Gomperts, R. E. Stratmann, O. Yazyev, A. J. Austin, R. Cammi, C. Pomelli, J. W. Ochterski, R. L. Martin, K. Morokuma, V. G. Zakrzewski, G. A. Voth, P. Salvador, J. J. Dannenberg, S. Dapprich, A. D. Daniels, Ö. Farkas, J. B. Foresman, J. V. Ortiz, J. Cioslowski and D. J. Fox, *Journal*, 2009.
65. A. A. Skelton and J. R. Fried, *Physical Chemistry Chemical Physics*, 2013, **15**, 4341-4354.
66. T. H. Dunning, *Journal of Chemical Physics*, 1989, **90**, 1007-1023.
67. A. A. Skelton, V. M. Khedkar and J. R. Fried, *Journal of Biomolecular Structure and Dynamics*, In Print.
68. V. Zoete, M. A. Cuendet, A. Grosdidier and O. Michielin, *Journal of Computational Chemistry*, 2011, **32**, 2359-2368.
69. J. C. Phillips, R. Braun, W. Wang, J. Gumbart, E. Tajkhorshid, E. Villa, C. Chipot, R. D. Skeel, L. Kale and K. Schulten, *Journal of computational chemistry*, 2005, **26**, 1781-1802.
70. I. Dzidic and P. Kebarle, *Journal of Physical Chemistry*, 1970, **74**, 1466-&.
71. R. J. Wheatley, *Mol. Phys.*, 1996, **87**, 1083-1116.
72. S. M. Ali, *Comput. Theor. Chem.*, 2014, **1034**, 38-52.
73. D. Beglov and B. Roux, *Journal of Chemical Physics*, 1994, **100**, 9050-9063.
74. J. Chowdhary, E. Harder, P. E. M. Lopes, L. Huang, A. D. MacKerell and B. Roux, *The Journal of Physical Chemistry B*, 2013, **117**, 9142-9160.
75. T. R. Lucas, B. A. Bauer and S. Patel, *Biochimica et Biophysica Acta (BBA) - Biomembranes*, 2012, **1818**, 318-329.